The flavor-changing top-charm quark production in the littlest Higgs model with T parity at the ILC

Xuelei Wang,* Huiling Jin, Yanju Zhang, and Yanhui Xi

College of Physics and Information Engineering,
Henan Normal University, Xinxiang, Henan 453007. P.R. China

(Dated: March 20, 2008)

Abstract

With high luminosity and energy at the ILC and clean SM backgrounds, the top-charm production at the ILC should have powerful potential to probe new physics. The littlest Higgs model with discrete symmetry named "T-parity"(LHT) is one of the most promising new physics models. In this paper, we study the FC processes $e^+e^-(\gamma\gamma) \to t\bar{c}$ at the ILC in the LHT model. Our study shows that the LHT model can make a significant contribution to these processes. When the masses of mirror quarks become large, these two processes are accessible at the ILC. So the top-charm production at the ILC provides a unique way to study the properties of the FC couplings in the LHT model and furthermore test the model.

PACS numbers: 14.65.Ha,12.60.-i, 12.15.Mn,13.85.Lg

*Electronic address: wangxuelei@sina.com

I. INTRODUCTION

A simple doublet scalar field yields a perfectly appropriate gauge symmetry breaking pattern in the Standard Model(SM). On the other hand, its theoretical shortcomings, such as quadratic divergencies(hierarchy problem) or the triviality of a ϕ^4 theory suggest that it is embedded in a larger scheme. Recently, an alternative known as the little Higgs mechanism[1], has been propased. Such mechanism that makes the Higgs "little" in the current reincarnation of the PGB idea is collective symmetry breaking. Collective symmetry breaking protects the Higgs by several symmetries under each of which the Higgs is an exact Goldstone. Only if the symmetries are broken collectively, i.e. by more than one coupling in the theory, can the Higgs pick up a contribution to its mass and hence all one-loop quadratic divergences to the Higgs mass are avoided. The most compact implementation of the little Higgs mechanism is known as the littlest Higgs model[2]. In this model, the SM is enlarged to incorporate an approximate $SU(5)$ global symmetry. This symmetry is broken down to $SO(5)$ spontaneously, though the mechanism of this breaking is left unspecified. The Higgs is an approximate Goldstone boson of this breaking. In this model there are new vector bosons, a heavy top quark and a triplet of heavy scalars in addition to the SM particles. These new particles can make significant tree-level contributions to the experimental observables. So the original LH model suffers strong constraints from electroweak precision data[3]. The most serious constraints result from the tree-level corrections to precision electroweak observables due to the exchanges of the additional heavy gauge bosons, as well as from the small but non-vanishing vacuum expectation value(VEV) of the additional weak-triplet scalar field. To solve this problem, a Z_2 discrete symmetry named "T-parity" is introduced[4]. The littlest Higgs model with T parity(LHT), requires the introduction of "mirror fermions" for each SM fermion doublet. The mirror fermions are odd under T-parity and can be given large masses and the SM fields are T-even. T parity explicitly forbids any tree-level contribution from the heavy gauge bosons to the observables involving only standard model particles as external states. It also forbids the interactions that induce the triplet VEV. As a result, in the LHT model, corrections to precision electroweak observables are generated at loop-level. This implies that the constraints are generically weaker than in the tree-level case, and fine tuning can be avoided[5]. In the LHT model, one of the important ingredients of the mirror sector is the existence of CKM-like unitary mixing matrices. These mirror mixing matrices parameterize flavor-changing(FC) interactions between the SM fermions and the mirror fermions. Such new FC interactions have a very different pattern from ones present in the SM and can have significant contributions to some FC processes. As we know, the SM does not contain the tree-level FC neutral currents, though it can occur at higher order through radiative corrections. Because of the loop suppression, these SM FC effects are hardly to be observed. So this stimulates a lot of efforts in probing new physics via FC processes[6, 7, 8, 9, 10, 11]. The impact of the FC interactions in the LHT on FC processes such as neutral meson mixing and rare K, B meson decays are studied in Refs.[10]. The FC couplings between the SM fermions and the mirror fermions can also induce the loop-level $tcV(V = \gamma, Z, g)$ couplings. The rare top quark decays $t \to cV$ in the LHT model have been studies in Ref.[11] and the study shows that the decays $t \to cV$ in the LHT model can be significantly enhanced relative to those in the SM. The FC couplings tcV can also make contributions to the top-charm production. In this paper, we will systematically study the contribution of the FC couplings in the LHT

model to the top-charm production at the ILC, i.e., $e^+e^-(\gamma\gamma) \to t\bar{c}$. The motivations to study the FC top-charm production are as follows:(1)The LHT model is an ideal idea to solve the hierarchy problem and does not suffer from severe constraints from precision electroweak measurewments. (2)Due to the extreme suppression in the SM, the top-charm production can provide the clean SM background to probe the quantum effect of the LHT model. (3)Due to its rather clean environment and high luminosity, the International Linear Collider(ILC) will be an ideal machine to probe new physics. In such a collider, in addition to e^+e^- collision, we can also realize photon-photon collision. The FC top-charm production at the ILC will be a sensitive probe for different new physics models and one might distinguish different new physics models with the precise measurement of these processes at the ILC.

This paper is organized as follows. In Sec.II, we briefly review the LHT model. Sec.III presents the detailed calculation of the production cross sections of the processes. The numerical results are shown in Sec.IV. We present discussions and conclusions in the last section.

II. A BRIEF REVIEW OF THE LHT MODEL

The LH model embeds the electroweak sector of the SM in an $SU(5)/SO(5)$ non-linear sigma model. It begins with a global $SU(5)$ symmetry with a locally gauged sub-group $[SU(2) \times U(1)]^2$. The $SU(5)$ symmetry is spontaneously broken down to $SO(5)$ via a VEV of order f. At the same time, the $[SU(2) \times U(1)]^2$ gauge symmetry is broken to its diagonal subgroup $SU(2)_L \times U(1)_Y$ which is identified as the SM electroweak gauge group. From the $SU(5)/SO(5)$ breaking, there arise 14 Nambu-Goldstone bosons which are described by the matrix Π, given explicitly by

$$\Pi = \begin{pmatrix} -\frac{\omega^0}{2} - \frac{\eta}{\sqrt{20}} & -\frac{\omega^+}{\sqrt{2}} & -i\frac{\pi^+}{\sqrt{2}} & -i\phi^{++} & -i\frac{\phi^+}{\sqrt{2}} \\ -\frac{\omega^-}{\sqrt{2}} & \frac{\omega^0}{2} - \frac{\eta}{\sqrt{20}} & \frac{v+h+i\pi^0}{2} & -i\frac{\phi^+}{\sqrt{2}} & \frac{-i\phi^0+\phi^P}{\sqrt{2}} \\ i\frac{\pi^-}{\sqrt{2}} & \frac{v+h-i\pi^0}{2} & \sqrt{4/5}\eta & -i\frac{\pi^+}{\sqrt{2}} & \frac{v+h+i\pi^0}{2} \\ i\phi^{--} & i\frac{\phi^-}{\sqrt{2}} & i\frac{\pi^-}{\sqrt{2}} & -\frac{\omega^0}{2} - \frac{\eta}{\sqrt{20}} & -\frac{\omega^-}{\sqrt{2}} \\ i\frac{\phi^-}{\sqrt{2}} & \frac{i\phi^0+\phi^P}{\sqrt{2}} & \frac{v+h-i\pi^0}{2} & -\frac{\omega^+}{\sqrt{2}} & \frac{\omega^0}{2} - \frac{\eta}{\sqrt{20}} \end{pmatrix} \tag{1}$$

Here, $H = (-i\pi^+\sqrt{2}, (v + h + i\pi^0)/2)^T$ plays the role of the SM Higgs doublet, i.e. h is the usual Higgs field, $v = 246$ GeV is the Higgs VEV, and $\pi^\pm, \pi^0$ are the Goldstone bosons associated with the spontaneous symmetry breaking $SU(2)_L \times U(1)_Y \to U(1)_{em}$. The fields η and ω are additional Goldstone bosons eaten by heavy gauge bosons when the $[SU(2) \times U(1)]^2$gauge group is broken down to $SU(2)_L \times U(1)_Y$. The field Φ is a physical scalar triplet with

$$\Phi = \begin{pmatrix} -i\phi^{++} & -i\frac{\phi^+}{\sqrt{2}} \\ -i\frac{\phi^+}{\sqrt{2}} & \frac{-i\phi^0+\phi^P}{\sqrt{2}} \end{pmatrix} \tag{2}$$

Its mass is given by

$$m_\Phi = \sqrt{2} m_H \frac{f}{v}, \tag{3}$$

with m_H being the mass of the SM Higgs scalar.

In the LHT model, a T-parity discrete symmetry is introduced to make the model consistent with the electroweak precision data. Under the T-parity, the field Φ, ω, and η are odd, and the SM Higgs doublet H is even.

For the gauge group $[SU(2) \times U(1)]^2$, there are eight gauge bosons, $W_1^{a\mu}, B_1^{\mu}, W_2^{a\mu}, B_2^{\mu}$(a=1,2,3). A natural way to define the action of T-parity on the gauge fields is

$$W_1^a \Leftrightarrow W_2^a, \qquad B_1 \Leftrightarrow B_2. \tag{4}$$

An immediate consequence of this definition is that the gauge couplings of the two $SU(2)\times U(1)$ factors have to be equal.

The gauge boson T-parity eigenstates are given by

$$W_L^a = \frac{W_1^a + W_2^a}{\sqrt{2}}, \qquad B_L = \frac{B_1 + B_2}{\sqrt{2}} \quad (T-even) \tag{5}$$

$$W_H^a = \frac{W_1^a - W_2^a}{\sqrt{2}}, \qquad B_L = \frac{B_1 - B_2}{\sqrt{2}} \quad (T-odd) \tag{6}$$

From the first step of symmetry breaking $[SU(2) \times U(1)]^2 \rightarrow SU(2)_L \times U(1)_Y$, the T-odd heavy gauge bosons acquire masses. The masses of the T-even gauge bosons are generated only through the second step of symmetry breaking $SU(2)_L \times U(1)_Y \rightarrow U(1)_{em}$. Finally, the mass eigenstates are given at order $O(v^2/f^2)$ by

$$W_L^{\pm} = \frac{W_L^1 \mp iW_L^2}{\sqrt{2}}, \qquad W_H^{\pm} = \frac{W_H^1 \mp iW_H^2}{\sqrt{2}} \tag{7}$$

$$Z_L = cos\theta_W W_L^3 - sin\theta_W B_L, \qquad Z_H = W_H^3 + x_H \frac{v^2}{f^2} B_H, \tag{8}$$

$$A_L = sin\theta_W W_L^3 + cos\theta_W B_L, \qquad A_H = -x_H \frac{v^2}{f^2} W_H^3 + B_H, \tag{9}$$

where θ_W is the usual weak mixing angle and

$$x_H = \frac{5gg'}{4(5g^2 - g'^2)}, \tag{10}$$

with g, g' being the corresponding coupling constants of $SU(2)_L$ and $U(1)_Y$. The masses of the T-odd gauge bosons are given by

$$M_{Z_H} \equiv M_{W_H} = fg(1 - \frac{v^2}{8f^2}), \qquad M_{A_H} = \frac{fg'}{\sqrt{5}}(1 - 5\frac{v^2}{8f^2}), \tag{11}$$

The masses of the T-even gauge bosons are given by

$$M_{W_L} = \frac{gv}{2}(1 - \frac{v^2}{12f^2}), \qquad M_{Z_L} = \frac{gv}{2cos\theta_W}(1 - \frac{v^2}{12f^2}), M_{A_L} = 0. \tag{12}$$

A consistent and phenomenologically viable implementation of T-parity in the fermion sector requires the introduction of mirror fermions. The T-even fermion section consists

of the SM quarks, leptons and an additional heavy quark T_+. The T-odd fermion sector consists of three generations of mirror quarks and leptons and an additional heavy quark T_-. Only the mirror quarks (u_H^i, d_H^i) are involved in this paper. The mirror fermions get masses

$$m_{H_i}^u = \sqrt{2}\kappa_i f(1 - \frac{v^2}{8f^2}) \equiv m_{H_i}(1 - \frac{v^2}{8f^2}), \qquad (13)$$
$$m_{H_i}^d = \sqrt{2}\kappa_i f \equiv m_{H_i},$$

where the Yukawa couplings κ_i can in general depend on the fermion species i.

The mirror fermions induce a new flavor structure and there are four CKM-like unitary mixing matrices in the mirror fermion sector:

$$V_{H_u}, \quad V_{H_d}, \quad V_{H_l}, \quad V_{H_\nu}. \qquad (14)$$

These mirror mixing matrices are involved in the FC interactions between the SM fermions and the T-odd mirror fermions which are mediated by the T-odd heavy gauge bosons or the Goldstone bosons. V_{H_u} and V_{H_d} satisfy the relation

$$V_{H_u}^\dagger V_{H_d} = V_{CKM}. \qquad (15)$$

We parameterize the V_{H_d} with three angles $\theta_{12}^d, \theta_{23}^d, \theta_{13}^d$ and three phases $\delta_{12}^d, \delta_{23}^d, \delta_{13}^d$

$$V_{H_d} = \begin{pmatrix} c_{12}^d c_{13}^d & s_{12}^d s_{13}^d e^{-i\delta_{12}^d} & s_{13}^d e^{-i\delta_{13}^d} \\ -s_{12}^d c_{23}^d e^{i\delta_{12}^d} - c_{12}^d s_{23}^d s_{13}^d e^{i(\delta_{13}^d - \delta_{23}^d)} & c_{12}^d c_{23}^d - s_{12}^d s_{23}^d s_{13}^d e^{i(\delta_{13}^d - \delta_{12}^d - \delta_{23}^d)} & s_{23}^d c_{13}^d e^{-i\delta_{23}^d} \\ s_{12}^d s_{23}^d e^{i(\delta_{12}^d + \delta_{23}^d)} - c_{12}^d c_{23}^d s_{13}^d e^{i\delta_{13}^d} & -c_{12}^d s_{23}^d e^{i\delta_{23}^d} - s_{12}^d c_{23}^d s_{13}^d e^{i(\delta_{13}^d - \delta_{12}^d)} & c_{23}^d c_{13}^d \end{pmatrix} \qquad (16)$$

The matrix V_{H_u} is then determined through $V_{H_u} = V_{H_d} V_{CKM}^\dagger$. As in the case of the CKM matrix the angles θ_{ij}^d can all be made to lie in the first quadrant with $0 \leq \delta_{12}^d, \delta_{23}^d, \delta_{13}^d < 2\pi$.

III. THE TOP-CHARM PRODUCTION IN THE LHT MODEL

A. The loop-level FC couplings $tcZ(\gamma)$ in the LHT model

As we have mentioned above, there are FC interactions between SM fermions and T-odd mirror fermions which are mediated by the T-odd heavy gauge bosons$(A_H, Z_H, W_H^\pm)$ or Goldstone bosons$(\eta, \omega^0, \omega^\pm,)$. The relevant Feynman rules can be found in Ref.[10]. With these FC couplings, the loop-level FC couplings $tcZ(\gamma)$ can be induced and the relevant Feynman diagrams are shown in Fig.1.

As we know, each diagram in Fig.1 actually contains ultraviolet divergence. Because there is no corresponding tree-level $tcZ(\gamma)$ couplings to absorb these divergences, the divergences just cancel each other and the total effective $tcZ(\gamma)$ couplings are finite as they should be. The effective one loop-level couplings $tcZ(\gamma)$ can be directly calculated based on Fig.1. Their explicit forms, $\Gamma_{tc\gamma}^\mu(p_t, p_c)$ and $\Gamma_{tcZ}^\mu(p_t, p_c)$, are given in Appendix.

The study has shown that the FC couplings $tcV(V = Z, \gamma, g)$ can largely enhance the branching ratios of rare top quark decays $t \to cV$[11]. On the other hand, the couplings can also contribute to the top-charm production via the processes $e^+e^-(\gamma\gamma) \to t\bar{c}$. We will discuss these processes in the following.

B. The calculation of the cross sections for the processes $e^+e^-(\gamma\gamma) \to t\bar{c}$ in the LHT model

In the LHT model, the existence of the FC couplings $tcZ(\gamma)$ can induce the process $e^+e^- \to t\bar{c}$ at loop-level. The corresponding Feynman diagram is shown in Fig.2(A).

The production amplitudes are

$$M_A = M_A^\gamma + M_A^Z,$$

with

$$M_A^\gamma = -eG(p_1+p_2,0)\bar{u}_t(p_3)\Gamma^u_{tc\gamma}(p_3,p_4)v_{\bar{c}}(p_4)\bar{v}_{e^+}(p_2)\gamma_u u_{e^-}(p_1), \tag{17}$$

$$\begin{aligned} M_A^Z &= \frac{g}{\cos\theta_W}G(p_1+p_2,M_Z)\bar{u}_t(p_3)\Gamma^u_{tcZ}(p_3,p_4)v_{\bar{c}}(p_4)\bar{v}_{e^+}(p_2)\gamma_u \\ &\quad [(-\frac{1}{2}+\sin^2\theta_W)P_L + (\sin^2\theta_W)P_R]u_{e^-}(p_1). \end{aligned} \tag{18}$$

Where $P_L = \frac{1}{2}(1-\gamma_5)$ and $P_R = \frac{1}{2}(1+\gamma_5)$ are the left and right chirality projectors. p_1, p_2 are the momenta of the incoming e^+, e^-, and p_3, p_4 are the momenta of the outgoing final states top quark and anti-charm quark, respectively. We also define $G(p,m)$ as $\frac{1}{p^2-m^2}$.

On the other hand, a unique feature of the ILC is that it can be transformed to $\gamma\gamma$ collision with the photon beams generated by using the Compton backscattering of the initial electron and laser beams. In this case, the energy and luminosity of the photon beams would be the same order of magnitude of the original electron beams, and the set of final states at a photon collider is much richer than that in the e^+e^- mode. So the realization of the photon collider will open a wider window to probe new physics. In the LHT model, the top-charm quarks can also be produced through $\gamma\gamma$ collision, and the relevant Feynman diagrams are shown in Fig.2(B-C). The invariant production amplitudes of the process $\gamma\gamma \to t\bar{c}$ can be written as:

$$M_B = -\frac{2e}{3}G(p_3-p_1,m_c)\bar{u}_t(p_3)\Gamma^\mu_{tc\gamma}(p_3,p_3-p_1)\epsilon_\mu(p_1)(\not{p}_3-\not{p}_1+m_c)\not{\epsilon}(p_2)\nu_{\bar{c}}(p_4), \tag{19}$$

$$M_C = -\frac{2e}{3}G(p_2-p_4,m_t)\bar{u}_t(p_3)\not{\epsilon}(p_1)(\not{p}_2-\not{p}_4+m_t)\Gamma^\nu_{tc\gamma}(p_2-p_4,p_4)\epsilon_\nu(p_2)\nu_{\bar{c}}(p_4). \tag{20}$$

With the above amplitudes M_B, M_C, we can directly obtain the production cross section $\hat{\sigma}(\hat{s})$ for the subprocess $\gamma\gamma \to t\bar{c}$ and the total cross sections at the e^+e^- linear collider can be obtained by folding $\hat{\sigma}(\hat{s})$ with the photon distribution function $F(x)$ which is given in Ref.[12],

$$\sigma_{tot}(s) = \int_{x_{min}}^{x_{max}} dx_1 \int_{x_{min}x_{max}/x_1}^{x_{max}} dx_2 F(x_1)F(x_2)\hat{\sigma}(\hat{s}), \tag{21}$$

where s is the c.m. energy squared for e^+e^-. The subprocess occur effectively at $\hat{s} = x_1x_2s$, and x_i are the fractions of the electron energies carried by the photons. The explicit form of the photon distribution function $F(x)$ is

$$F(x) = \frac{1}{D(\xi)}\left[1-x+\frac{1}{1-x}-\frac{4x}{\xi(1-x)}+\frac{4x^2}{\xi^2(1-x)^2}\right], \tag{22}$$

with

$$D(\xi) = \left(1 - \frac{4}{\xi} - \frac{8}{\xi^2}\right) \ln(1+\xi) + \frac{1}{2} + \frac{8}{\xi} - \frac{1}{2(1+\xi)^2}, \tag{23}$$

and

$$\xi = \frac{4E_0\omega_0}{m_e^2}. \tag{24}$$

E_0 and ω_0 are the incident electron and laser light energies, and $x = \omega/E_0$. The energy ω of the scattered photon depends on its angle θ with respect to the incident electron beam and is given by

$$\omega = \frac{E_0(\frac{\xi}{1+\xi})}{1 + (\frac{\theta}{\theta_0})^2}. \tag{25}$$

Therefore, at $\theta = 0$, $\omega = E_0\xi/(1+\xi) = \omega_{max}$ is the maximum energy of the backscattered photon, and $x_{max} = \frac{\omega_{max}}{E_0} = \frac{\xi}{1+\xi}$.

To avoid unwanted e^+e^- pair production from the collision between the incident and back-scattered photons, we should not choose too large ω_0. The threshold for e^+e^- pair creation is $\omega_{max}\omega_0 > m_e^2$, so we require $\omega_{max}\omega_0 \leq m_e^2$. Solving $\omega_{max}\omega_0 = m_e^2$, we find

$$\xi = 2(1+\sqrt{2}) = 4.8. \tag{26}$$

For the choice $\xi = 4.8$, we obtain $x_{max} = 0.83$ and $D(\xi_{max}) = 1.8$. The minimum value for x is determined by the production threshold

$$x_{min} = \frac{\hat{s}_{min}}{x_{max}s}, \quad \hat{s}_{min} = (m_t + m_c)^2. \tag{27}$$

Here we have assumed that both photon beams and electron beams are unpolarized. We also assume that, the number of the backscattered photons produced per electron is one.

IV. THE NUMERICAL RESULTS OF THE PROCESSES $e^+e^-(\gamma\gamma) \to t\bar{c}$ IN THE LHT MODEL

To obtain numerical results of the cross sections, we calculate the amplitudes numerically by using the method of reference[13], instead of calculating the square of the production amplitudes analytically. This greatly simplifies our calculations.

There are several free parameters in the LHT model which are involved in the production amplitudes. They are the breaking scale f, the masses of the mirror quarks $m_{H_i}(i = 1, 2, 3)$(Here we have ignored the masses difference between up-type mirror quarks and down-type mirror quarks), and 6 parameters($\theta_{12}^d,\ \theta_{13}^d,\ \theta_{23}^d,\ \delta_{12}^d,\ \delta_{13}^d,\ \delta_{23}^d$) which are related to the mixing matrix V_{H_d}. In Ref.[10], the constraints on the mass spectrum of the mirror fermions have been investigated from the analysis of neutral meson mixing in the K, B and D systems. They found that a TeV scale GIM suppression is necessary

for a generic choice of V_{H_d}. However, there are regions of parameter space where are only very loose constraints on the mass spectrum of the mirror fermions. Here we study the processes $e^+e^-(\gamma\gamma) \to t\bar{c}$ based on the two scenarios for the structure of the matrix V_{H_d}, as in Ref.[11]. i.e.,

Case I: $V_{H_d} = 1, \quad V_{H_u} = V_{CKM}^\dagger$,
Case II: $s_{23}^d = 1/\sqrt{2}, \quad s_{12}^d = s_{13}^d = 0, \quad \delta_{12}^d = \delta_{23}^d = \delta_{13}^d = 0.$

In both cases, the constraints on the mass spectrum of the mirror fermions are very relaxed. For the breaking scale f, we take two typical values: 500 GeV and 1000 GeV.

To get the numerical results of the cross sections, we should also fix some parameters in the SM as m_t =174.2 GeV, m_c =1.25 GeV, s_W^2 =0.23, M_Z =91.87 GeV, $\alpha_e = 1/128$, and $v = 246$ GeV[14]. For the c.m. energies of the ILC, we choose $\sqrt{s} = 500,\ 1000$ GeV as examples. On the other hand, taking account of the detector acceptance, we have taken the basic cuts on the transverse momentum(p_T) and the pseudo-rapidity(η) for the final state particles

$$p_T \geq 20GeV, \qquad |\eta| \leq 2.5.$$

The numerical results of the processes $e^+e^-(\gamma\gamma) \to t\bar{c}$ are summarized in Figs.3-5, and the anti-top production is also included in our calculation. In Figs.3-4, we plot the cross sections of the processes $e^+e^-(\gamma\gamma) \to t\bar{c}$ as a function of M_{H_3} for case I and case II, respectively. In case I, the mixing in the down type gauge and Goldstone boson interactions are absent. In this case there are no constraints on the masses of the mirror quarks at one loop-level from the K and B systems and the constraints come only from the D system. The constraints on the mass of the third generation mirror quark are very weak[10]. For Case I, we take m_{H_3} to vary in the range of 500-5000 GeV, and fix $m_{H_1} = m_{H_2}$=300 GeV. We can see from Fig.3 that both cross sections of the processes $e^+e^- \to t\bar{c}$ and $\gamma\gamma \to t\bar{c}$ rise very fast with the m_{H_3} increasing. This is because the couplings between the mirror quarks and the SM quarks are proportion to the masses of the mirror quarks. The dependences of c.m. energy $\sqrt{s}$ on the cross sections are different between the two processes. For the process $e^+e^- \to t\bar{c}$, the contributions of the LHT model come from s-channel, so the large c.m. energy $\sqrt{s}$ depresses the cross section. However, the LHT model makes t-channel contributions to the process $\gamma\gamma \to t\bar{c}$ and the large c.m. energy can enhance its cross section. The masses of the heavy gauge bosons and the mirror quarks, M_{V_H} and m_{H_i}, are proportion to f, but the scale f is insensitive to the cross sections of both processes because the production amplitudes are represented in the form of m_{H_i}/M_{V_H}. For Case II, the dependence of the cross sections on m_{H_3} is presented in Fig.4. In this case, the constraints from the K and B systems are also very weak. Compared to Case I, the mixing between the second and third generations are enhanced with the choice of a bigger mixing angle s_{23}^d. Even with stricter constraints on the masses of the mirror quarks, the large masses of the mirror quarks can also enhance the cross sections significantly. The dependence of the cross sections on the c.m. energy is similar to that in Case I. In both Case I and case II, the cross section of $\gamma\gamma \to t\bar{c}$ is several orders of magnitude larger than that of $e^+e^- \to t\bar{c}$. So the process $\gamma\gamma \to t\bar{c}$ benefits from a large cross section.

In order to provide more information for ILC experiments to probe the LHT model via the top-charm production, we also give out the transverse momentum distributions of the top quark in Fig.5. We fix $\sqrt{s} = 500$ GeV, $f = 500$ GeV, $m_{H_1} = m_{H_2} = 300$

GeV, $m_{H_3} = 2500$ GeV for Case I and fix $\sqrt{s} = 500$ GeV, $f = 500$ GeV, $m_{H_1} = m_{H_2} = 1000$ GeV, $m_{H_3} = 1500$ GeV for Case II. We can see that the p_t^T distributions of two processes are very different. The p_t^T distribution of the process $e^+e^- \to t\bar{c}$ increases with p_t^T increasing, but the p_t^T distribution of the process $\gamma\gamma \to t\bar{c}$ decreases sharply with p_t^T. These two processes can provide complementary information in different transverse momentum space.

V. DISCUSSIONS AND CONCLUSIONS

Due to the GIM mechanism, the top quark FC interactions are absent at tree-level and extremely small at loop-level. So the production rate of $t\bar{c}$ process is very small in the SM and such process can not be observed. In some new physics models, there exist new FC interactions which can enhance the cross section of top-charm production significantly. So the study of top-charm production would play an important role in probing new physics models. In the LHT model, there exist the FC couplings between the SM fermions and mirror fermions which can make large loop-level contributions to the couplings $tcZ(\gamma)$ and greatly enhance the production rates of the $t\bar{c}$ processes at the ILC. In this paper, we study the processes $e^+e^-(\gamma\gamma) \to t\bar{c}$ in the framework of the LHT model at the ILC. We find that the cross sections of these two processes vary in a very wide range within the parameter space limited by the neutral meson mixing in the K, B and D systems. With heavy mirror quarks, the cross sections of $e^+e^-(\gamma\gamma) \to t\bar{c}$ become very large, specially for the process $\gamma\gamma \to t\bar{c}$, but for relative light mirror quarks the cross sections become very small. If these processes can be observed and their cross sections can be measured at the ILC, up-limits on the masses of the mirror quarks can be obtained. If these processes can not be observed, relative light mirror quarks are favorable by data of the ILC. Much more $t\bar{c}$ events can be obtained via photon-photon collision. So more detail information about the FC couplings in the LHT model should be obtained via $\gamma\gamma \to t\bar{c}$.

VI. ACKNOWLEDGMENTS

We would thank Junjie Cao for useful discussions and providing the calculation programs. This work is supported by the National Natural Science Foundation of China under Grant No.10775039, 10575029 and 10505007.

[1] N. Arkani-Hamed, A. G. Cohen and H. Georgi, *Phys. Lett.* B**513**, 232(2001).

[2] N. Arkani-Hamed, A. G. Cohen, E. Katz, A. E. Nelson, *JHEP* **0207**, 034(2002).

[3] J. L. Hewett, F. J. Petriello, and T. G. Rizzo, *JHEP* **0310**, 062(2003); C. Csaki, J. Hubisz, G. D. Kribs, P. Meade, and J. Terning, *Phys.Rev.* D**67**, 115002(2003).

[4] I. Low, *JHEP*, **0410**, 067(2004); H. C. Cheng and I. Low, *JHEP*, **0408**, 061(2004); J. Hubisz and P.Meade, *Phys.Rev.* D**71**, 035016(2005); J. Hubisz, S. J. Lee and G. Paz, *JHEP*, **0606**, 041(2006).

[5] J. Hubisz, P. Meade, A. Noble, and M. Perelstein, *JHEP* **0601**, 136(2006).

[6] H. J. He, C. P. Yuan, *Phys.Rev.Lett.* **83**, 28(1999); G. Burdman, *Phys.Rev.Lett.* **83**, 2888(1999).

[7] For FCNC top-quark decay, see, X. L. Wang et.al., *Phys.Rev.* D**50**, 5781(1994); C. Yue et.al., *Phys.Lett.* B**508**, 290(2001); G. R. Lu, F. R. Yin, X. L. Wang, L. D. Wan, *Phys.Rev.* D**68**, 015002(2003); C. S. Li, R. J. Oakes, J. M. Yang, *Phys.Rev.* D**49**, 293(1994); G. Couture, C. Hamzaoui, H. Konig, *Phys.Rev.* D**52**, 1713(1995); J. L. Lopez, D. V. Nanopoulos, R. Rangarajan, *Phys.Rev.* D**56**, 3100(1997); G. M. de Divitiis, R. Petronzio, L. Silvestrini, *Nucl. Phys.* B**504**, 45(1997); J. M. Yang, B.-L. Young, X.Zhang,*Phys.Rev.* D**58**, 055001(1998); J. M. Yang, C. S. Li, *Phys.Rev.* D**49**, 3412(1994); J. Guasch, J. Sola,*Nucl. Phys.* B**562**, 3(1999); G. Eilam et al., *Phys.Lett.* B**510**, 227(2001); J. J. Liu, C. S. Li, L. L. Yang, L. G. Jin, *Phys.Lett.* B**599**, 92(2004).

[8] For top-charm productions, see, J. Cao, Z. Xiong, J. M. Yang, *Nucl. Phys.* B**651**, 87(2003); C. S. Li, X. Zhang, S. H. Zhu, *Phys. Rev.* D**60**, 077702(1999); J. J. Liu, C. S. Li, L. L.Yang, L. G. Jin, *Nucl. Phys.* B**705**, 3(2005); Z. H. Yu, H. Pietschmann, W. G. Ma, L. Han, Y. Jiang, *Eur. Phys.* J. C**16**, 541(2000); Y. Jiang, M. L. Zhou, W. G. Ma, L. Han, H. Zhou, M. Han, *Phys.Rev.* D**57**, 4343(1994); C. Yue, Y. Dai, Q. Xu, G. Liu, *Phys.Lett.* B**525**, 301(2002); C. Yue, G. Liu, Q. Xu, *Phys.Lett.* B**509**, 294(2002); C. Yue, G. Lu, J. Cao, J. Li, G. Liu, *Phys.Lett.* B**496**, 93(2000); J. Cao, Z. Xiong, J. M. Yang, *Phys.Rev.* D**67**, 071701(2003).

[9] X. L. Wang, Y. L. Yang, B. Z. Li, C. X. Yue, J. Y. Zhang, *Phys.Rev.* D**66**, 075009(2002); X. L. Wang, B. Z. Li, Y. L. Yang, *Phys.Rev.* D**68**, 115003(2003); W. N. Xu, X. L. Wang, Z. J. Xiao, *Eur. Phys. J.* C**51** 891(2007).

[10] J. Hubisz, S. J. Lee, and G. Paz, *JHEP* **0606**, 041(2006); M. Mlanke, A. J. Buras, A. Poschenrieder, C. Tarantino, S. Uhlig and A. Weiler, *JHEP* **0612**, 003(2006); M. Mlanke, A. J. Buras, A. Poschenrieder, S. Recksiegel, C. Tarantino, S. Uhlig and A. Weiler, *JHEP* **0611**, 062(2006).

[11] H. S. Hou, hep-ph/0703067

[12] G. Jikia, *Nucl. Phys.* B**374**, 83(1992); O. J. P. Eboli, et al., *Phys. Rev.* D**47**, 1889(1993); K. M. Cheung, *ibid.* **47**, 3750 (1993).

[13] K. Hagiwara and D. Zeppenfeld, *Nucl. Phys.* B**313**, 560(1989); V. Barger, T. Han and D. Zeppenfeld, *Phys. Rev.* D**41**, 2782(1990).

[14] Particle Data Group, W. -M. Yao *et al.*, *J.Phys.* G**33** 1(2006).

Appendix: The explicit expressions of the effective $tcZ(\gamma)$ couplings $\Gamma^{\mu}_{tc\gamma},\ \Gamma^{\mu}_{tcZ}$

The effective $tcZ(\gamma)$ couplings $\Gamma^{\mu}_{tc\gamma},\ \Gamma^{\mu}_{tcZ}$ can be directly calculated based on Fig.1, and they can be represented in form of 2-point and 3-point standard functions B_0, B_1, C_{ij}. Due to $m_t >> m_c$, we have safely ignored the terms m_c/m_t in the calculation. On the other hand, the high order $1/f^2$ terms in the masses of new gauge bosons and in the Feynman rules are also ignored. $\Gamma^{\mu}_{tc\gamma}$ and Γ^{μ}_{tcZ} are depended on the momenta of top quark and charm quark(p_t, p_c). Here p_t is outgoing and p_c is incoming. The explicit expressions of $\Gamma^{\mu}_{tc\gamma},\ \Gamma^{\mu}_{tcZ}$ are

$$\begin{aligned}
\Gamma^{\mu}_{tc\gamma}(p_t,p_c) &= \Gamma^{\mu}_{tc\gamma}(\eta^0)+\Gamma^{\mu}_{tc\gamma}(\omega^0)+\Gamma^{\mu}_{tc\gamma}(\omega^{\pm})+\Gamma^{\mu}_{tc\gamma}(A_H)+\Gamma^{\mu}_{tc\gamma}(Z_H)+\Gamma^{\mu}_{tc\gamma}(W_H^{\pm})\\
&\quad +\Gamma^{\mu}_{tc\gamma}(W_H^{\pm}\omega^{\pm}),
\end{aligned}$$

$$\begin{aligned}
\Gamma^{\mu}_{tc\gamma}(\eta^0) &= \frac{i}{16\pi^2}\frac{eg'^2}{150M^2_{A_H}}(V_{Hu})_{3i}(V_{Hu})_{i2}m^2_{Hi}\\
&\quad \{[B_0(-p_t,m_{Hi},0)-B_0(-p_c,m_{Hi},0)+B_1(-p_t,m_{Hi},0)\\
&\quad +2C^a_{24}-2p_t\cdot p_c(C^a_{12}+C^a_{23})+m^2_t(C^a_{21}+C^a_{11}+C^a_0)-m^2_{Hi}C^a_0]\gamma^{\mu}P_L\\
&\quad +[-2m_t(C^a_{21}+2C^a_{11}+C^a_0)]p^{\mu}_tP_L+[2m_t(C^a_{23}+2C^a_{12})]p^{\mu}_cP_L\},
\end{aligned}$$

$$\begin{aligned}
\Gamma^{\mu}_{tc\gamma}(\omega^0) &= \frac{i}{16\pi^2}\frac{eg^2}{6M^2_{Z_H}}(V_{Hu})_{3i}(V_{Hu})_{i2}m^2_{Hi}\\
&\quad \{[B_0(-p_t,m_{Hi},0)-B_0(-p_c,m_{Hi},0)+B_1(-p_t,m_{Hi},0)\\
&\quad +2C^b_{24}-2p_t\cdot p_c(C^b_{12}+C^b_{23})+m^2_t(C^b_{21}+C^b_{11}+C^b_0)-m^2_{Hi}C^b_0]\gamma^{\mu}P_L\\
&\quad +[-2m_t(C^b_{21}+2C^b_{11}+C^b_0)]p^{\mu}_tP_L+[2m_t(C^b_{23}+2C^b_{12})]p^{\mu}_cP_L\},
\end{aligned}$$

$$\begin{aligned}
\Gamma^{\mu}_{tc\gamma}(\omega^{\pm}) &= \frac{i}{16\pi^2}\frac{eg^2}{6M^2_{W_H}}(V_{Hu})_{3i}(V_{Hu})_{i2}m^2_{Hi}\\
&\quad \{2[(B_0(-p_t,m_{Hi},0)-B_0(-p_c,m_{Hi},0)+B_1(-p_t,m_{Hi},0))\\
&\quad -2C^c_{24}+6C^g_{24}+2p_t\cdot p_c(C^c_{12}+C^c_{23})-m^2_t(C^c_{21}+C^c_{11}+C^c_0)+m^2_{Hi}C^c_0]\gamma^{\mu}P_L\\
&\quad +[2m_t(C^c_{21}+2C^c_{11}+C^c_0)+3m_t(2C^g_{21}+C^g_{11})]p^{\mu}_tP_L\\
&\quad +[-2m_t(C^c_{23}+2C^c_{12})-3m_t(2C^g_{23}+C^g_{11})]p^{\mu}_cP_L\},
\end{aligned}$$

$$\begin{aligned}
\Gamma^{\mu}_{tc\gamma}(A_H) &= \frac{i}{16\pi^2}\frac{eg'^2}{75}(V_{Hu})_{3i}(V_{Hu})_{i2}\\
&\quad \{[B_1(-p_t,m_{Hi},M_{A_H})+2C^d_{24}-2p_t\cdot p_c(C^d_{11}+C^d_{23})+m^2_t(C^d_{21}+C^d_{11})\\
&\quad -m^2_{Hi}C^d_0]\gamma^{\mu}P_L+[-2m_t(C^d_{21}+C^d_{11})]p^{\mu}_tP_L+[2m_t(C^d_{23}+C^d_{11})]p^{\mu}_cP_L\},
\end{aligned}$$

$$\begin{aligned}
\Gamma^{\mu}_{tc\gamma}(Z_H) &= \frac{i}{16\pi^2}\frac{eg^2}{3}(V_{Hu})_{3i}(V_{Hu})_{i2}\\
&\quad \{[B_1(-p_t,m_{Hi},M_{Z_H})+2C^e_{24}-2p_t\cdot p_c(C^e_{11}+C^e_{23})+m^2_t(C^e_{21}+C^e_{11})\\
&\quad -m^2_{Hi}C^e_0]\gamma^{\mu}P_L+[-2m_t(C^e_{21}+C^e_{11})]p^{\mu}_tP_L+[2m_t(C^e_{23}+C^e_{11})]p^{\mu}_cP_L\},
\end{aligned}$$

$$\Gamma^{\mu}_{tc\gamma}(W^{\pm}_H) = \frac{i}{16\pi^2}\frac{eg^2}{6}(V_{Hu})_{3i}(V_{Hu})_{i2}$$
$$\{[4B_1(-p_t, m_{Hi}, M_{W_H}) + 2B_0(p_c, m_{Hi}, M_{W_H}) - 4C^f_{24} + 4C^h_{24}$$
$$+4p_t\cdot p_c(C^f_{11} + C^f_{23}) - 2m_t^2(C^f_{21} + C^f_{11}) + 2m^2_{Hi}C^f_0 + 2M^2_{W_H}C^h_0$$
$$-4p_t\cdot p_c(C^h_{11} + C^h_0) + m_t^2(3C^h_{11} + C^h_0)]\gamma^{\mu}P_L$$
$$+[4m_t(C^f_{21} + C^f_{11}) + 2m_t(3C^h_{11} + 2C^h_{21} + C^h_0)]p^{\mu}_t P_L$$
$$+[-4m_t(C^f_{23} + C^f_{11}) - 2m_t(2C^h_{23} + 3C^h_{12} - C^h_{11} - C^h_0)]p^{\mu}_c P_L\},$$

$$\Gamma^{\mu}_{tc\gamma}(W^{\pm}_H\omega^{\pm}) = \frac{i}{16\pi^2}\frac{eg^2}{0}2(V_{Hu})_{3i}(V_{Hu})_{i2}$$
$$\{[m^2_{Hi}(C^i_0 - C^j_0) + m_t^2(C^j_{11} + C^j_0)]\gamma^{\mu}P_L + [-2m_tC^j_{12}]p^{\mu}_c P_L\}.$$

$$\Gamma^{\mu}_{tcZ}(p_t, p_c) = \Gamma^{\mu}_{tcZ}(\eta^0) + \Gamma^{\mu}_{tcZ}(\omega^0) + \Gamma^{\mu}_{tcZ}(\omega^{\pm}) + \Gamma^{\mu}_{tcZ}(A_H) + \Gamma^{\mu}_{tcZ}(Z_H) + \Gamma^{\mu}_{tcZ}(W^{\pm}_H)$$
$$+\Gamma^{\mu}_{tcZ}(W^{\pm}_H\omega^{\pm}),$$

$$\Gamma^{\mu}_{tcZ}(\eta^0) = \frac{i}{16\pi^2}\frac{g}{\cos\theta_W}(\frac{1}{2} - \frac{2}{3}\sin^2\theta_W)\frac{g'^2}{100M^2_{A_H}}(V_{Hu})_{3i}(V_{Hu})_{i2}m^2_{Hi}$$
$$\{[B_0(-p_t, m_{Hi}, 0) - B_0(-p_c, m_{Hi}, 0) + B_1(-p_t, m_{Hi}, 0)$$
$$+2C^a_{24} - 2p_t\cdot p_c(C^a_{12} + C^a_{23}) + m_t^2(C^a_{21} + C^a_{11} + C^a_0) - m^2_{Hi}C^a_0]\gamma^{\mu}P_L$$
$$+[-2m_t(C^a_{21} + 2C^a_{11} + C^a_0)]p^{\mu}_t P_L + [2m_t(C^a_{23} + 2C^a_{12})]p^{\mu}_c P_L\},$$

$$\Gamma^{\mu}_{tcZ}(\omega^0) = \frac{i}{16\pi^2}\frac{g}{\cos\theta_W}(\frac{1}{2} - \frac{2}{3}\sin^2\theta_W)\frac{g^2}{4M^2_{Z_H}}(V_{Hu})_{3i}(V_{Hu})_{i2}m^2_{Hi}$$
$$\{[B_0(-p_t, m_{Hi}, 0) - B_0(-p_c, m_{Hi}, 0) + B_1(-p_t, m_{Hi}, 0)$$
$$+2C^b_{24} - 2p_t\cdot p_c(C^b_{12} + C^b_{23}) + m_t^2(C^b_{21} + C^b_{11} + C^b_0) - m^2_{Hi}C^b_0]\gamma^{\mu}P_L$$
$$+[-2m_t(C^b_{21} + 2C^b_{11} + C^b_0)]p^{\mu}_t P_L + [2m_t(C^b_{23} + 2C^b_{12})]p^{\mu}_c P_L\},$$

$$\Gamma^{\mu}_{tcZ}(\omega^{\pm}) = \frac{i}{16\pi^2}\frac{g}{\cos\theta_W}\frac{g^2}{2M^2_{W_H}}(V_{Hu})_{3i}(V_{Hu})_{i2}m^2_{Hi}$$
$$\{[(\frac{1}{2} - \frac{2}{3}\sin^2\theta_W)(B_0(-p_t, m_{Hi}, 0) - B_0(-p_c, m_{Hi}, 0)$$
$$+B_1(-p_t, m_{Hi}, 0)) + (-\frac{1}{2} + \frac{1}{3}\sin^2\theta_W)(2C^c_{24} - 2p_t\cdot p_c(C^c_{12} + C^c_{23})$$
$$+m_t^2(C^c_{21} + C^c_{11} + C^c_0) - m^2_{Hi}C^c_0) + 2\cos^2\theta_W C^g_{24}]\gamma^{\mu}P_L$$
$$+[(-\frac{1}{2} + \frac{1}{3}\sin^2\theta_W)(-2m_t(C^c_{21} + 2C^c_{11} + C^c_0))$$
$$+\cos^2\theta_W m_t(2C^g_{21} + C^g_{11})]p^{\mu}_t P_L + [2(-\frac{1}{2} + \frac{1}{3}\sin^2\theta_W)m_t(C^c_{23} + 2C^c_{12})$$
$$-\cos^2\theta_W m_t(2C^g_{23} + C^g_{11})]p^{\mu}_c P_L\},$$

$$\Gamma^{\mu}_{tcZ}(A_H) = \frac{i}{16\pi^2}\frac{g}{\cos\theta_W}(\frac{1}{2}-\frac{2}{3}\sin^2\theta_W)\frac{g'^2}{50}(V_{Hu})_{3i}(V_{Hu})_{i2}$$
$$\{[B_1(-p_t,m_{Hi},M_{A_H})+2C^d_{24}-2p_t\cdot p_c(C^d_{11}+C^d_{23})+m_t^2(C^d_{21}+C^d_{11})$$
$$-m^2_{Hi}C^d_0]\gamma^{\mu}P_L+[-2m_t(C^d_{21}+C^d_{11})]p_t^{\mu}P_L+[2m_t(C^d_{23}+C^d_{11})]p_c^{\mu}P_L\},$$

$$\Gamma^{\mu}_{tcZ}(Z_H) = \frac{i}{16\pi^2}\frac{g}{\cos\theta_W}(\frac{1}{2}-\frac{2}{3}\sin^2\theta_W)\frac{g^2}{2}(V_{Hu})_{3i}(V_{Hu})_{i2}$$
$$\{[B_1(-p_t,m_{Hi},M_{Z_H})+2C^e_{24}-2p_t\cdot p_c(C^e_{11}+C^e_{23})+m_t^2(C^e_{21}+C^e_{11})$$
$$-m^2_{Hi}C^e_0]\gamma^{\mu}P_L+[-2m_t(C^e_{21}+C^e_{11})]p_t^{\mu}P_L+[2m_t(C^e_{23}+C^e_{11})]p_c^{\mu}P_L\},$$

$$\Gamma^{\mu}_{tcZ}(W^{\pm}_H) = \frac{i}{16\pi^2}\frac{g}{\cos\theta_W}g^2(V_{Hu})_{3i}(V_{Hu})_{i2}$$
$$\{[(\frac{1}{2}-\frac{2}{3}\sin^2\theta_W)B_1(-p_t,m_{Hi},M_{W_H})$$
$$+(-\frac{1}{2}+\frac{1}{3}\sin^2\theta_W)(2C^f_{24}-2p_t\cdot p_c(C^f_{11}+C^f_{23})+m_t^2(C^f_{21}+C^f_{11})-m^2_{Hi}C^f_0)$$
$$+\frac{1}{6}\cos^2\theta_W(2B_0(p_c,m_{Hi},M_{W_H})+4C^h_{24}-4p_t\cdot p_c(C^h_{11}+C^h_0)$$
$$+m_t^2(3C^h_{11}+C^h_0)+2M^2_{W_H}C^h_0)]\gamma^{\mu}P_L$$
$$+[(-\frac{1}{2}+\frac{1}{3}\sin^2\theta_W)(-2m_t(C^f_{21}+C^f_{11}))$$
$$+\frac{1}{3}\cos^2\theta_W m_t(2C^h_{21}+3C^h_{11}+C^h_0)]p_t^{\mu}P_L$$
$$+[2(-\frac{1}{2}+\frac{1}{3}\sin^2\theta_W)m_t(C^f_{23}+C^f_{11})$$
$$-\frac{1}{3}\cos^2\theta_W m_t(2C^h_{23}+3C^h_{12}-C^h_{11}-C^h_0)]p_c^{\mu}P_L\},$$

$$\Gamma^{\mu}_{tcZ}(W^{\pm}_H\omega^{\pm}) = \frac{i}{16\pi^2}g\cos\theta_W\frac{g^2}{2}(V_{Hu})_{3i}(V_{Hu})_{i2}$$
$$\{[m^2_{Hi}(C^i_0-C^j_0)+m_t^2(C^j_{11}+C^j_0)]\gamma^{\mu}P_L+[-2m_tC^j_{12}]p_c^{\mu}P_L\}$$

The three-point standard functions $C_0,\ C_{ij}$ are defined as

$$\begin{aligned}
C^a_{ij} &= C^a_{ij}(-p_t, p_c, m_{Hi}, 0, m_{Hi}),\\
C^b_{ij} &= C^b_{ij}(-p_t, p_c, m_{Hi}, 0, m_{Hi}),\\
C^c_{ij} &= C^c_{ij}(-p_t, p_c, m_{Hi}, 0, m_{Hi}),\\
C^d_{ij} &= C^d_{ij}(-p_t, p_c, m_{Hi}, M_{A_H}, m_{Hi}),\\
C^e_{ij} &= C^e_{ij}(-p_t, p_c, m_{Hi}, M_{Z_H}, m_{Hi}),\\
C^f_{ij} &= C^f_{ij}(-p_t, p_c, m_{Hi}, M_{W_H}, m_{Hi}),\\
C^g_{ij} &= C^g_{ij}(-p_t, p_c, 0, m_{Hi}, 0),\\
C^h_{ij} &= C^h_{ij}(-p_t, p_c, M_{W_H}, m_{Hi}, M_{W_H}),\\
C^i_{ij} &= C^i_{ij}(-p_t, p_c, M_{W_H}, m_{Hi}, 0),\\
C^j_{ij} &= C^j_{ij}(-p_t, p_c, 0, m_{Hi}, M_{W_H}).
\end{aligned}$$

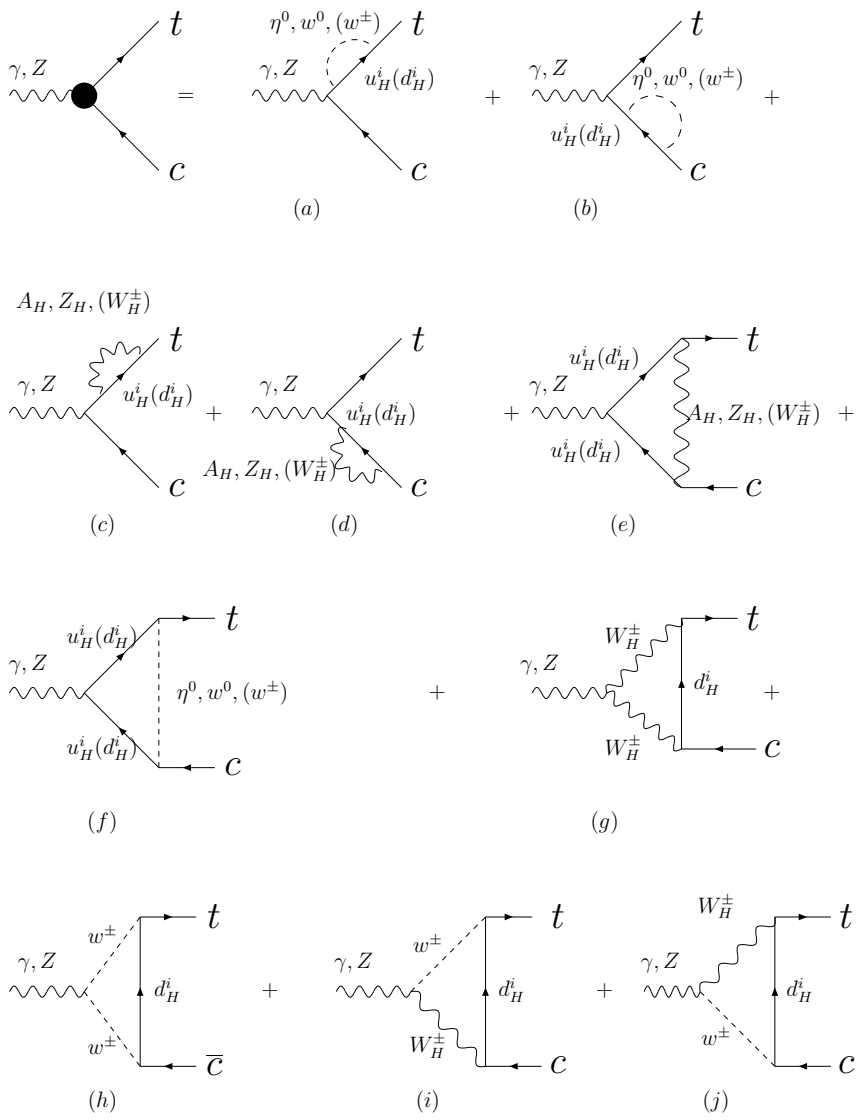

FIG. 1: The Feynman diagrams of the one-loop contributions of the LHC model to the couplings $tcZ(\gamma)$.

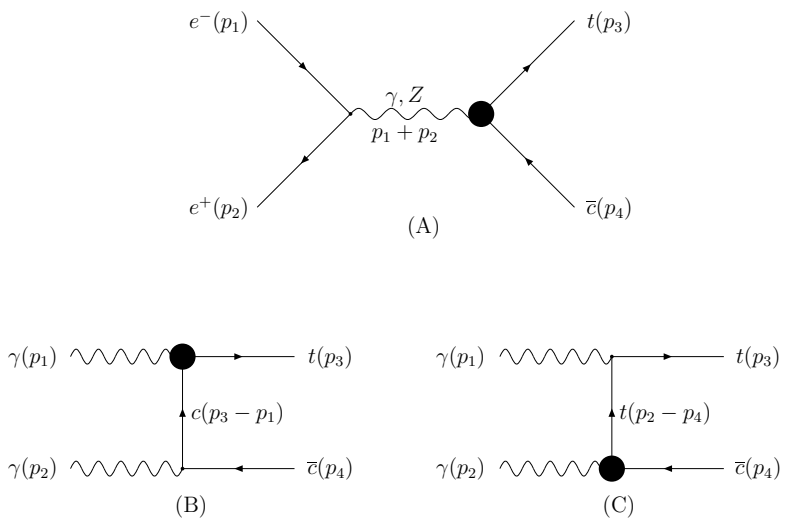

FIG. 2: The Feynman diagrams of the processes $e^+e^-(\gamma\gamma) \to t\bar{c}$ in the LHT model.

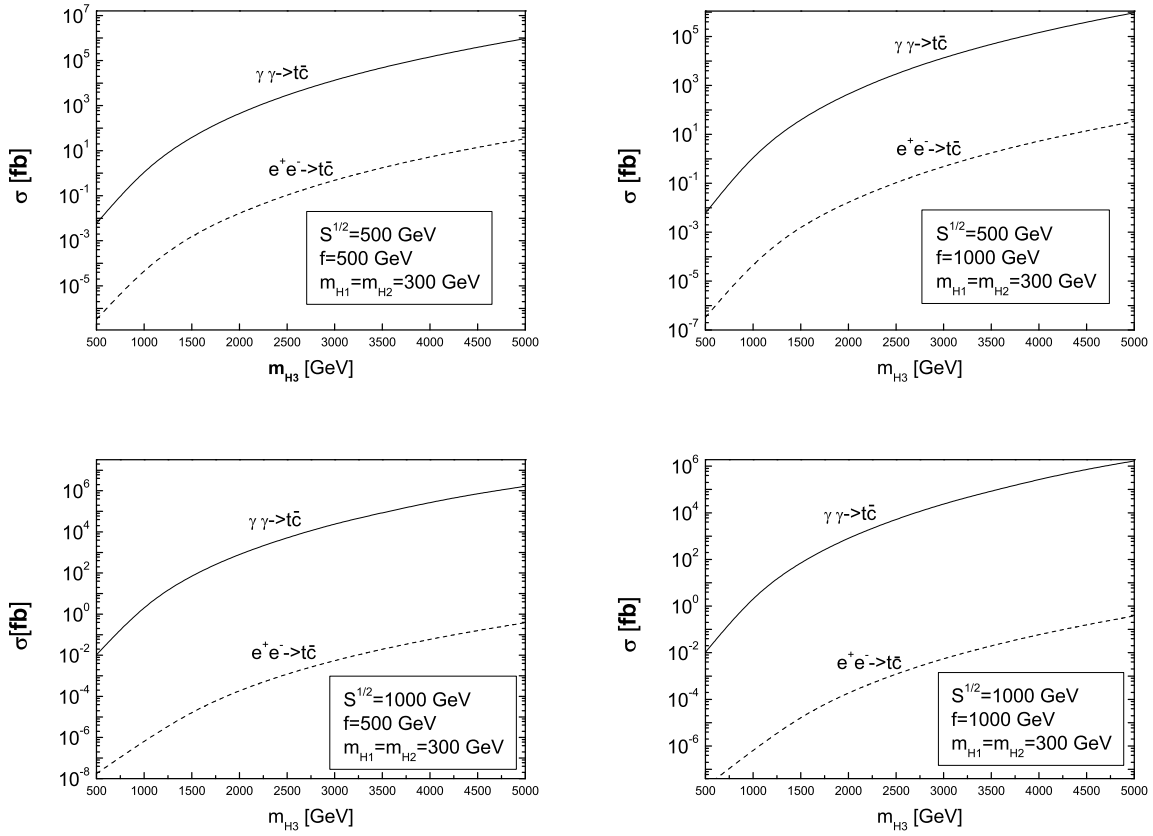

FIG. 3: The cross sections of the processes $e^+e^-(\gamma\gamma) \to t\bar{c}$ in the LHT model for Case I, as a function of M_{H_3}.

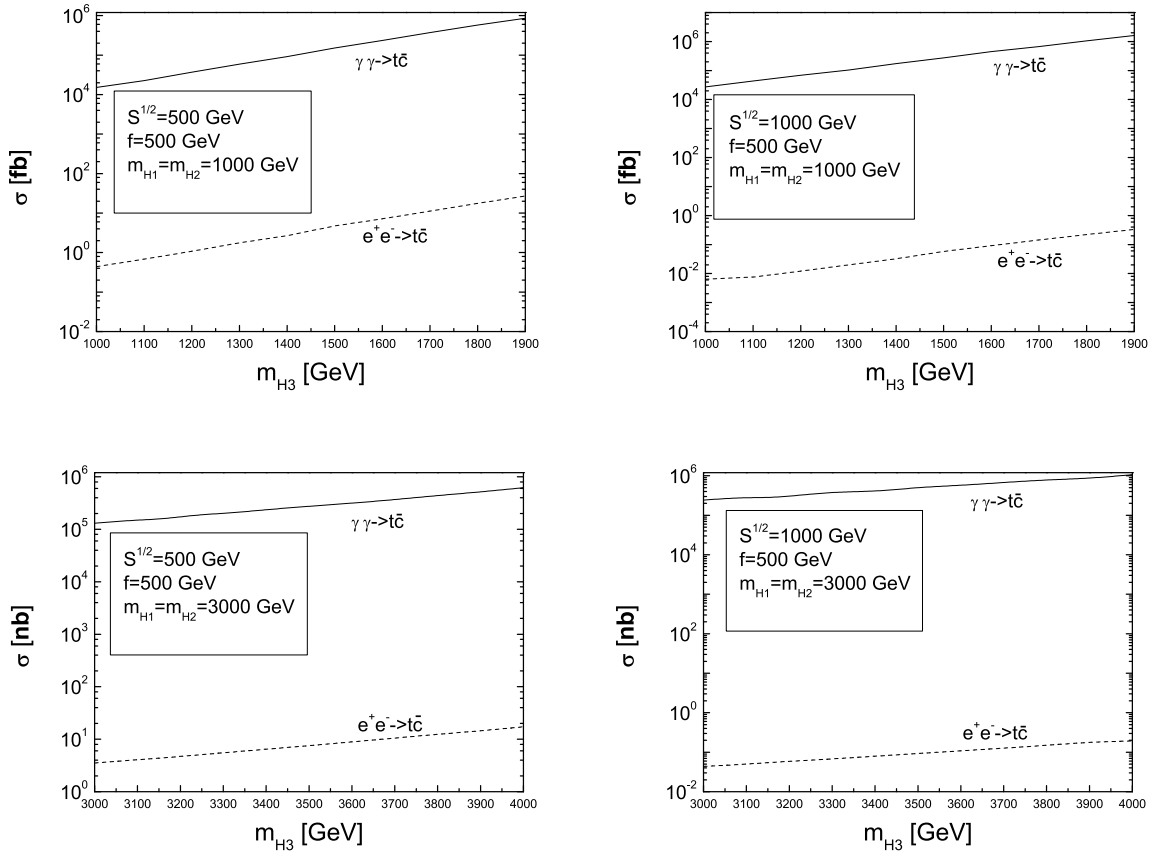

FIG. 4: The cross sections of the processes $e^+e^-(\gamma\gamma) \to t\bar{c}$ in the LHT model for Case II , as a function of M_{H_3}.

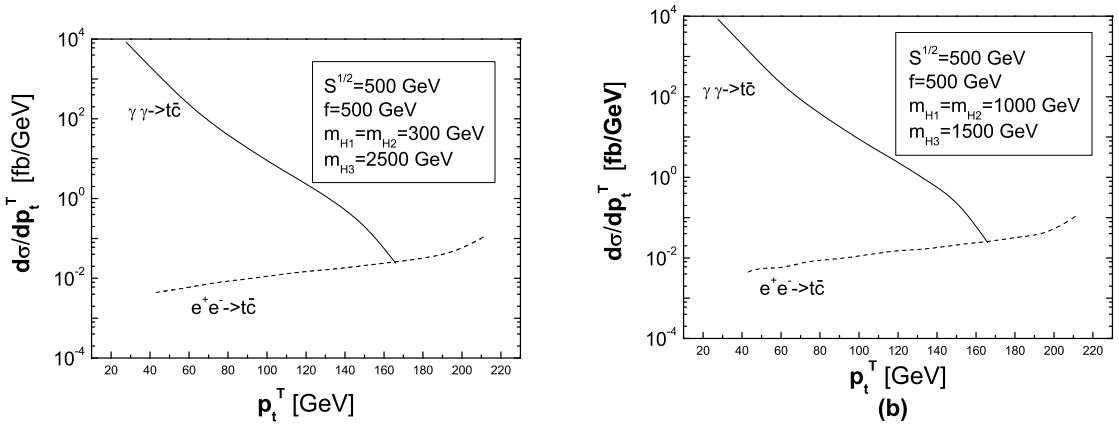

FIG. 5: The transverse momentum distributions of the top quark for the processes $e^+e^-(\gamma\gamma) \to t\bar{c}$ in the LHT model. The left diagram is for Case I and the right diagram is for Case II.